

Contents

1–2

Personal report

Michael T. Bowers Curriculum Vitae

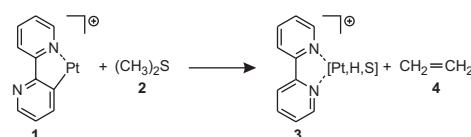
Regular articles

3–8

Platinum(II)-mediated dehydrosulfurization and oxidative carbon–carbon coupling in the gas-phase decomposition of thioethers

Burkhard Butschke, Maria Schlangen, Detlef Schröder, Helmut Schwarz

It is accordingly suggested that the (bipy–H)–ligand does not only affect the electronic structure of the platinum(II) core but, moreover, plays an active role as an acceptor in the initial hydrogen transfer from the thioether ligand to the LPt^+ core (L = heterocyclic ligand).

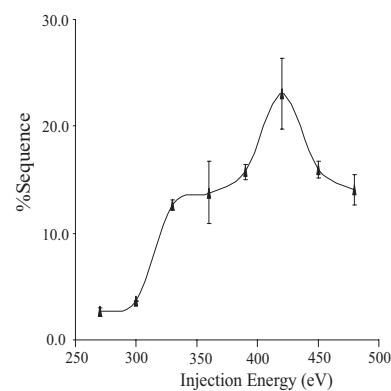


9–16

Charge state dependent fragmentation of gaseous α -synuclein cations via ion trap and beam-type collisional activation

Chamnongsak Chanthamontri, Jian Liu, Scott A. McLuckey

Ions derived from nano-electrospray ionization (nano-ESI) of α -synuclein, a 14.5 kDa, 140 amino acid residue protein that is a major component of the Lewy bodies associated with Parkinson's disease, have been subjected to ion trap and beam-type collisional activation.

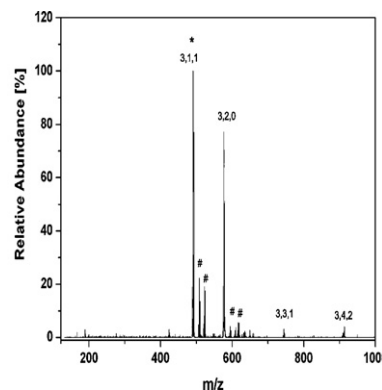


17–25

Role of cluster size and substrate in the gas phase C–C bond coupling reactions of allyl halides mediated by Ag_n^+ and $\text{Ag}_{n-1}\text{H}^+$ cluster cations

Farrah Qiuyun Wang, George N. Khairallah, Richard A.J. O'Hair

Here the influence of both the nature and the size of the silver cluster cation and the substrate on C–C bond coupling are examined.

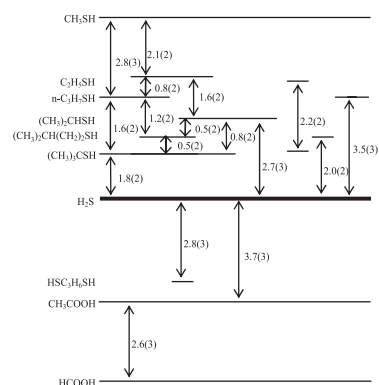


26–29

Anchoring the gas-phase acidity scale: From formic acid to methanethiol

Nicole Eyet, Stephanie M. Villano, Veronica M. Bierbaum

We have measured the gas-phase acidities of nine compounds: formic acid, acetic acid, 1,3-propanedithiol, 2-methyl-2-propanethiol, 3-methyl-1-butanethiol, 2-propanethiol, 1-propanethiol, ethanethiol, and methanethiol, with acidities ranging from 338.6 to 351.1 kcal mol⁻¹ using proton transfer kinetics and the resulting equilibrium constants.

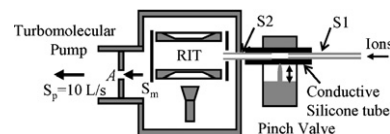


30–34

Characterization of a discontinuous atmospheric pressure interface. Multiple ion introduction pulses for improved performance

Liang Gao, Guangtao Li, Zongxiu Nie, Jason Duncan, Zheng Ouyang, R. Graham Cooks

In this study, the influence of the interface flow conductance and the mass spectrometer pumping speed on ion introduction into a handheld mass spectrometer is investigated.

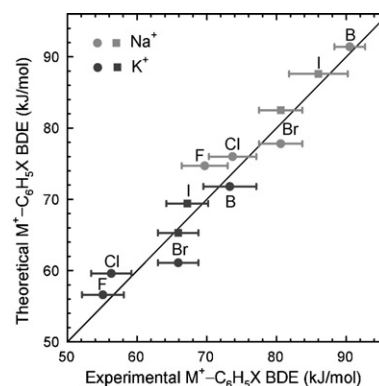


35–47

Inductive effects on cation– π interactions: Structures and bond dissociation energies of alkali metal cation–halobenzene complexes

Nuwan Hallowita, Estima Udonkang, Chunhai Ruan, C.E. Frieler, M.T. Rodgers

The influence of halogenation on cation– π interactions is investigated both experimentally and theoretically.

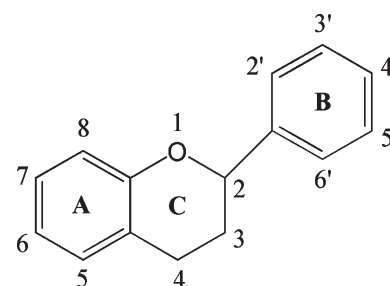


48–55

A study of the non-covalent interaction between flavonoids and DNA triplexes by electrospray ionization mass spectrometry

Cuihong Wan, Meng Cui, Fengrui Song, Zhiqiang Liu, Shuying Liu

The binding interactions of 22 flavonoids (9 aglycones and 13 glycosides) with DNA triplexes were investigated using electrospray ionization mass spectrometry (ESI-MS).

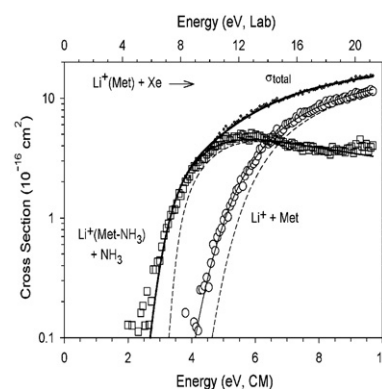


56–68

An experimental and theoretical study of alkali metal cation/methionine interactions

P.B. Armentrout, Amy Gabriel, R.M. Moision

The interactions of alkali metal cations ($M^+ = \text{Li}^+, \text{Na}^+, \text{K}^+$) with the amino acid methionine (Met) are examined in detail.

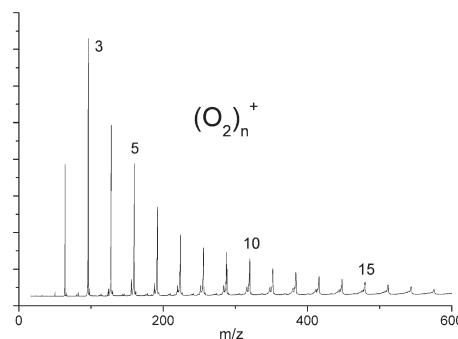


69–76

IR photodissociation spectroscopy of O_4^+ , O_6^+ and O_8^+ cluster ions

A.M. Ricks, G.E. Douberly, M.A. Duncan

O_4^+ and larger $(\text{O}_2)_n^+$ cluster ions are produced in a pulsed discharge source and studied with time-of-flight mass spectrometry and infrared laser photodissociation spectroscopy.

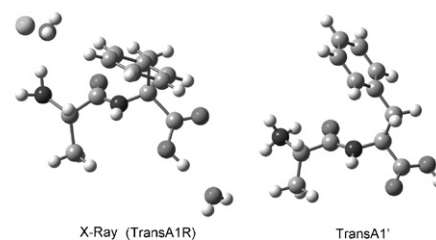


77–84

Gas-phase infrared spectroscopy of the protonated dipeptides H^+PheAla and H^+AlaPhe compared to condensed-phase results

Robert C. Dunbar, Jeffrey D. Steill, Nick C. Polfer, Jos Oomens

The gas-phase IRMPD spectrum of H^+AlaPhe shows that the gas-phase conformation differs from the crystalline chloride salt with respect to orientation of the terminal carboxyl

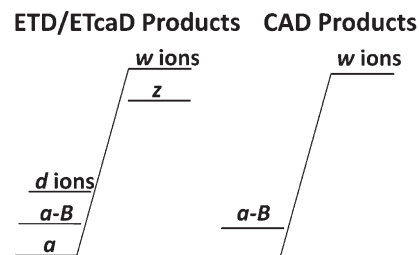


85–93

Electron transfer dissociation of oligonucleotide cations

Suncerae I. Smith, Jennifer S. Brodbelt

Electron transfer collision activated dissociation (ETcaD) of multi-protonated oligonucleotides results in an array of products with few base loss ions and internal fragments.

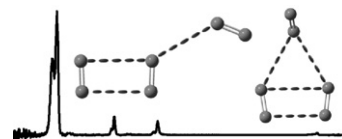


94–99

Vibrational predissociation spectra of the O_n^- , $n=3-10$, 12 clusters: Even-odd alternation in the core ion

Joseph C. Bopp, Anastassia N. Alexandrova, Ben M. Elliott, Tobias Herden, Mark A. Johnson

Anionic clusters of oxygen (O_n^-), formed in a supersonic free jet, build basically neutral solvent shells upon an ionic core.

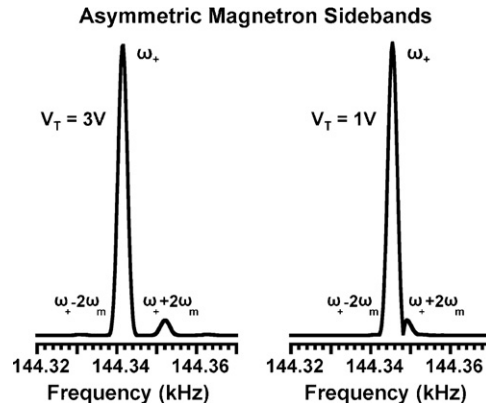


100–104

SIMION modeling of ion image charge detection in Fourier transform ion cyclotron resonance mass spectrometry

Christopher L. Hendrickson, Steven C. Beu, Greg T. Blakney, Alan G. Marshall

A SIMION model accurately calculates ion image charge detection in FT-ICR mass spectrometry that reveals nonlinear spectral features including ICR harmonics, trapping sidebands, and asymmetric magnetron sidebands.

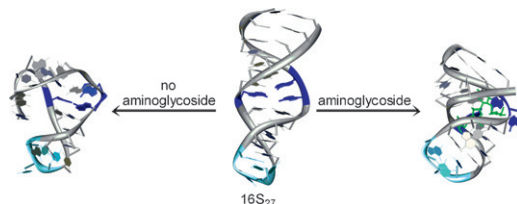


105–111

Aminoglycoside antibiotics: A-site specific binding to 16S

Erin Shammel Baker, Nicholas F. Dupuis, Michael T. Bowers

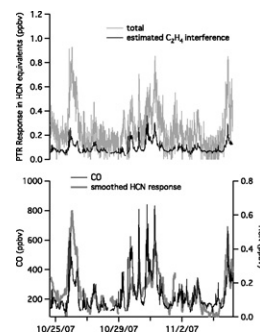
ESI-MS, ion mobility and molecular dynamics methods were utilized in this study to analyze the A-site of 16S₂₇ before and after the addition of ribostamycin (R), paromomycin (P) and lividomycin (L).



112–121**HCN detection with a proton transfer reaction mass spectrometer**

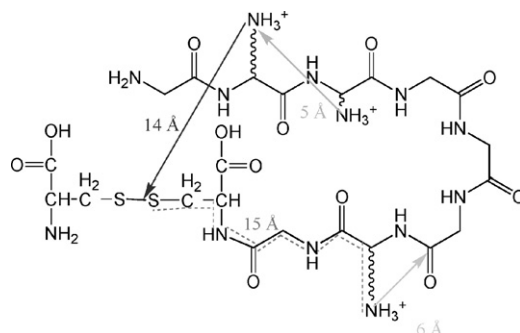
W.B. Knighton, E.C. Fortner, Anthony J. Midey, A.A. Viggiano,
S.C. Herndon, E.C. Wood, C.E. Kolb

A calibration method allowing for the accurate quantification of HCN with a PTR-MS using the $\text{H}_3\text{O}^+(\text{H}_2\text{O})_n$ distribution as a measure of water vapor concentration is described and demonstrated.

**122–134****Electron shuttling in electron transfer dissociation**

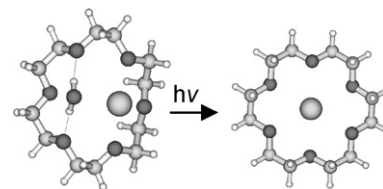
Diane Neff, Sylwia Smuczynska, Jack Simons

This paper describes theoretical efforts to understand how electrons attach to and fragment S–S and N–C $_{\alpha}$ bonds in peptides under ETD or ECD conditions.

**135–139****Infrared spectroscopy of gas-phase hydrated K⁺:18-crown-6 complexes: Evidence for high energy conformer trapping using the argon tagging method**

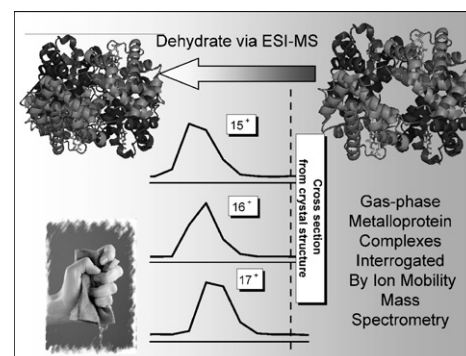
Jason D. Rodriguez, James M. Lisy

Argon tagging allows for the trapping of a high energy conformer which undergoes rearrangement upon photoexcitation by an IR photon.

**140–148****Gas-phase metalloprotein complexes interrogated by ion mobility-mass spectrometry**

Peter A. Faull, Karoliina E. Korkeila, Jason M. Kalapothakis, Andrew Gray,
Bryan J. McCullough, Perdita E. Barran

Ion mobility-mass spectrometry is employed to study the conformations of metalloproteins in the gas phase. Results give insight to subunit assembly and are compared to conformations from crystal structures.

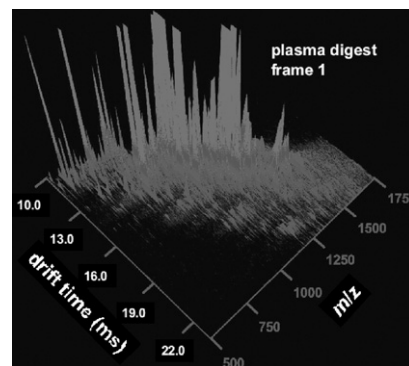


149–160

Developing IMS–IMS–MS for rapid characterization of abundant proteins in human plasma

Stephen J. Valentine, Ruwan T. Kurulugama, Brian C. Bohrer, Samuel I. Merenbloom, Renā A. Sowell, Yehia Mechref, David E. Clemmer

High-throughput comparative profiling (4 min) of plasma digest samples is demonstrated using IMS–IMS–MS techniques.

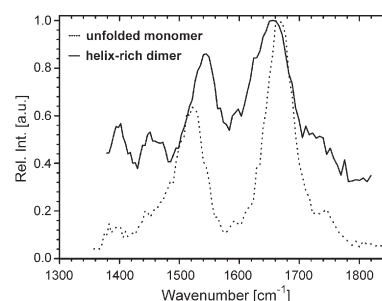


161–168

Gas-phase IR spectra of intact α -helical coiled coil protein complexes

Kevin Pagel, Peter Kupser, Frauke Bierau, Nicolas C. Polfer, Jeffrey D. Steill, Jos Oomens, Gerard Meijer, Beate Koks, Gert von Helden

Infrared multiphoton dissociation spectroscopy was employed to analyze the secondary structure of non-covalently associated α -helical coiled coil protein complexes in the gas phase.

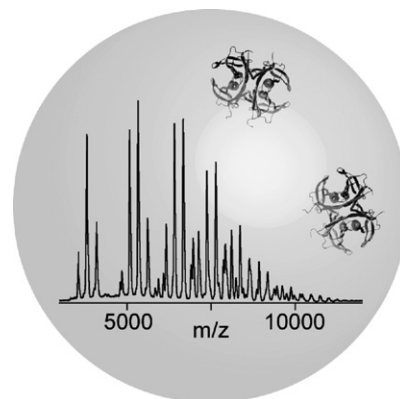


169–177

A Monte Carlo approach for assessing the specificity of protein oligomers observed in nano-electrospray mass spectra

Laura A. Lane, Brandon T. Ruotolo, Carol V. Robinson, Giorgio Favrin, Justin L.P. Benesch

Assessing the occupancy of nanospray droplets allows the determination of whether protein assemblies observed in the gas phase are reflective of their populations in solution.

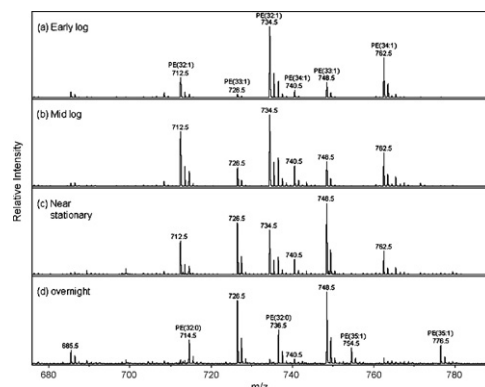


178–184

Lipid compositions in *Escherichia coli* and *Bacillus subtilis* during growth as determined by MALDI-TOF and TOF/TOF mass spectrometry

Jennifer Gidden, Jackie Denson, Rohana Liyanage, D. Mack Ivey, Jackson O. Lay Jr.

Lipids extracted from *E. coli* and *B. subtilis* during various stages of growth were analyzed by MALDI-TOF and TOF/TOF mass spectrometry.

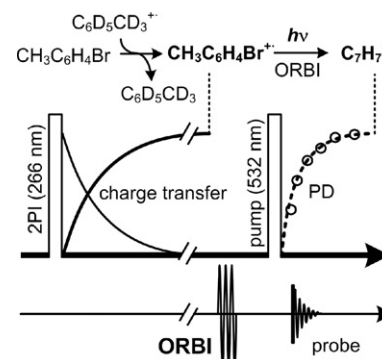


185–190

Collisional activation of ions by off-resonance irradiation in ion cyclotron resonance spectrometry

Seung Koo Shin, Seung-Jin Han, Jongcheol Seo

The effects of transient off-resonance burst irradiation on collisional activation of ions in the ICR cell were studied by time-resolved photodissociation spectroscopy and trajectory simulations.

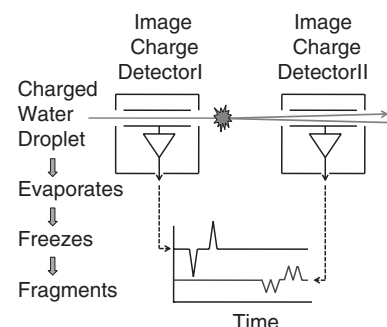


191–199

Freezing, fragmentation, and charge separation in sonic sprayed water droplets

Lloyd W. Zilch, Joshua T. Maze, John W. Smith, Martin F. Jarrold

Studies with two image charge detectors separated by a drift region show that micron sized water droplets fragment and change their charge while traveling through vacuum.

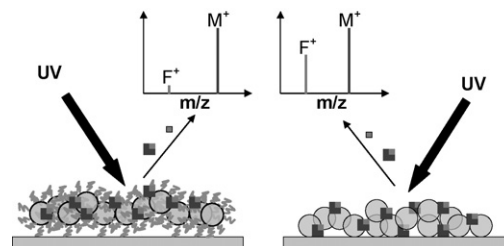


200–205

Internal energy deposition with silicon nanoparticle-assisted laser desorption/ionization (SPALDI) mass spectrometry

Shai Dagan, Yimin Hua, Dylan J. Boday, Arpad Somogyi, Ronald J. Wysocki, Vicki H. Wysocki

We report on a comparative study of internal energy deposition in silicon nanoparticle-assisted laser desorption/ionization (SPALDI). The internal energy deposition with silicon nanoparticles modified with fluorodecyl silane is slightly lower than with α -cyano-4-hydroxycinnamic acid (CHCA) and much lower than that deposited by untreated silicon nanoparticles. The internal energy deposition decreases with an increase in the chain length of the linear fluoro-alkyl modifier on the particles.

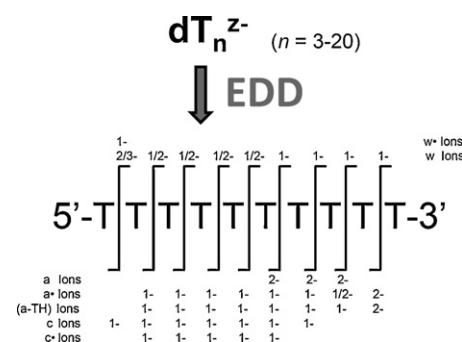


206–213

Electron detachment dissociation (EDD) pathways in oligonucleotides

Catherine Kinet, Valérie Gabelica, Dorothée Balbeur, Edwin De Pauw

We studied electron detachment dissociation (EDD) of oligonucleotides by double resonance in an FTICRMS to compare the fragmentation pathways with other radical-induced dissociation methods.

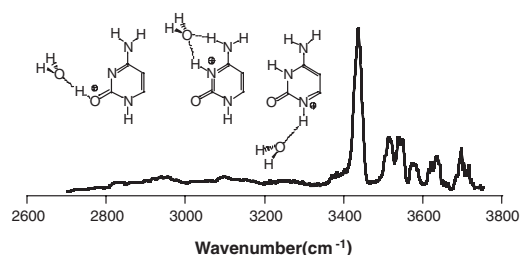


214–221

Tautomerism of cytosine probed by gas phase IR spectroscopy

Joost M. Bakker, Jean-Yves Salpin, Philippe Maître

Gas phase spectroscopy in the 2700–3750 cm⁻¹ IR range of singly hydrated complexes of protonated cytosine provides direct evidence for the coexistence of both C(2)=O and N(3) tautomers.

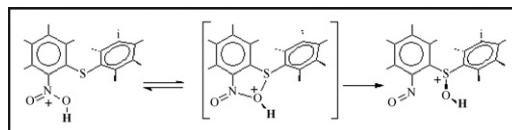


222–228

2-Nitrophenyl aryl sulfides undergo both intramolecular and electrostatic-induced intermolecular oxidation of sulfur: An experimental and theoretical case study

Joseph T. Moolayil, M. George, Daryl Giblin, Michael L. Gross

The intramolecular oxidation via oxygen transfer from the nitro group to the sulfur was corroborated by molecular modeling.



The Publisher encourage the submission of articles in electronic form thus saving time and avoiding rekeying errors.
Please refer to the online version of the Guide for Authors at <http://www.elsevier.com/locate/maspec>